Green's-function calculation of the surface properties of a two-band crystal*

W. Ho,† S. L. Cunningham,‡ and W. H. Weinberg
Division of Chemistry and Chemical Engineering, California Institute of Technology, Pasadena, California 91125

L. Dobrzynski
Laboratoire de Physique des Solides, Institut Supérieur d'Electronique du Nord, 3 rue Francois Baës, 59046 Lille Cedex, France
(Received 27 January 1975)

The electronic properties of the clean (001) surface of three model crystals with the CsCl structure have been calculated. One model results in no surface states, the second model yields Shockley surface states, and the third model yields Tamm surface states. Analytic expressions for both the bulk-crystal Green's function and the (001)-surface Green's function are derived. Using the resolvent technique, the surface-state bands are presented. Using the phase-shift technique, the change in the total density of states (both inside and outside of the bands) due to the creation of the surface are calculated. From this, the change in the specific heat due to the surface and the surface entropy are found. Finally, the local densities of states for the layers near the surface are obtained from the surface Green's function and compared with the local density of states in the bulk. Our results, which can be used to understand the properties of both semi-conductor and insulator surfaces, are contrasted with previous results for one-band crystal surfaces which are appropriate only for metals.

I. INTRODUCTION

Chemical and physical processes which occur at a solid surface depend critically upon the electronic structure of the surface layer of atoms. For example, adatoms which chemisorb to the surface interact with the first layer of atoms. In addition, the presence of surface states can cause the electronic energy bands to bend and thereby alter the electrical conductivity in the suface region. In order to understand these processes from a fundamental point of view, we must start with the study of the electronic structure of the clean surface. In a later paper,[1] we will build on the results of this paper and consider the problem of chemisorption and reconstruction.

In this paper we are concerned with the electronic properties of the clean (001) surface of a three-dimensional two-component crystal which has the CsCl structure [two interpenetrating simple cubic (sc) lattices]. We use the linear-combination-of-atomic-orbitals (LCAO) formalism within the limits of the tight-binding (TB) approximation. The Green's function (or resolvent) is determined for the bulk crystal as well as the perturbation required to create the surface. Then the phase-shift function is calculated from which the change in the electronic density of states due to the perturbation can be found. In addition, we find the surface Green's function from which we obtain the density of states for each layer in the crystal. Each aspect of this calculation is reviewed briefly below.

There is a long history, reviewed by Koutecky[2] and by Davison and Levine,[3] of the use of the LCAO and TB approximations for studying surface properties. In 1939, Goodwin[4] first used the method to study a finite monatomic linear chain. He found that electronic surface states (where the wave function and charge density are localized near the chain ends) were present only if the energy of the orbital on the end atoms was altered by more than a critical amount. Later, Hoffmann and Konya[5] studied the same system without the restriction of the TB approximation.

Use of the LCAO method on mixed linear crystals started in 1951 with the work of Hoffmann.[6] He considered the bulk properties of an infinite chain of the type A_nB_m, where n and m are arbitrary integers. Later, Amos and Davison[7] examined the surface properties of the simpler AB-type chain. For the infinite chain, there are two energy bands separated by an energy gap. As in the work of Goodwin,[4] they found that the electron orbital energy on the surface atoms must be perturbed in order to get surface states. Their surface states (called outer states) fell either above the top band or below the bottom band. More general work by Davison and Koutecky[8] found that surface states could also appear in the band gap (inner states) for certain types of perturbations.

Levine and Davison[9] compared qualitatively the results from a one-dimensional LCAO chain calculation to real binary systems such as NaCl, CdS, and GaAs. They assumed the chain to be made up of alternating s-like and p-like atoms. This model, unlike those previously considered, gives the band-gap minimum at the center of the

Brillouin zone rather than at the zone edge. They found that surface states appeared in the band gap even without perturbing the electron orbital energies of the end atoms. Thus the LCAO method can give rise to the two general types of surface states: namely, the Tamm state where a perturbation near the surface is required, and the Shockley state where no perturbation is needed. In addition to the study of surface states, the LCAO formalism has been used to study more subtle properties of one-dimensional systems. As an example, Cunningham and Maradudin[10] have recently used the LCAO approach to calculate the surface induced dynamic effective charge near the ends of a finite chain.

The LCAO-TB formalism has also been applied to three-dimensional systems using three different techniques. One important technique which was used by Koutecky and Tomasek[11] first solves for the bulk electronic energy levels as a function of the general complex wave vector. The allowed values of the wave vector are then determined by satisfying the appropriate boundary conditions; namely, the wave function in the crystal must match smoothly onto a decaying wave function in the vacuum. This technique of wave-function matching has been used widely in studying surface states,[12] but since it does not generally use the LCAO formalism, we will not mention it further.

Another important technique which is used widely is based on the observation by Goodwin[13] that for each wave-vector component parallel to the surface, the three-dimensional problem takes on the same form as the one-dimensional problem. This has led to a series of papers dealing with slab systems in which the crystal is infinite in extent in two directions but finite (typically less than 20 layers) in the third direction. Then for each wave-vector component, an eigenvalue matrix of managable size (size is determined by the product of the number of orbitals per atom and the number of layers in the slab) is obtained. Work using this technique has appeared by Pugh,[14] Hirabayashi,[15] Alstrup,[16,17] and more recently by Pandey and Phillips.[18,19] With the exception of work by Joannopolous and Cohen[20] on GaAs, the use of the LCAO technique with slab calculations has been confined to single-component crystals of the diamond structure. Many other slab calculations have been done,[21] but they do not use the LCAO approach.

These two techniques give information about the energy and wave function of the surface states for various components of the two-dimensional wave vector parallel to the surface. They do not, however, allow one to determine the change in the bulk density of states upon creating the surface, nor do they allow one to study the density-of-state changes which occur in chemisorption. This information is important in the study of photoemission and the study of heterogeneous catalysis, and it can be obtained by the third technique (the one we use in this paper).

The third technique for using the LCAO formalism for studying the surface of three-dimensional systems is known as the Green's function or resolvent technique. The details of this method will be discussed in Sec. III. Baldock[22] used this approach (which is due to Lifshitz) to combine the Green's-function method with the LCAO model. Then Koster and Slater[23] generalized the method and applied it to the study of impurity levels and end effects of simple one-dimensional systems. Koutecky and Davison[24] applied the technique to a general mixed one-dimensional crystal where the unit cell is composed of an arbitrary number of atoms of an arbitrary type. They demonstrated how both Tamm and Shockley surface states can arise. Thus, the situation now is that the surface electronic properties of one-dimensional systems are well understood.

Concerning three-dimensional systems, the resolvent method has been used by Koutecky,[25] Holland,[26] and Brown[27] to discuss formally the properties of surface states. Tomasek[28] applied the method to the study of the (111) surface of silicon and by using several simplifications performed the entire calculation analytically. Later, Freeman[29] showed how the resolvent method can be applied to more realistic systems by performing numerical calculations. Then Levine and Freeman[30] applied the technique to the surface of a crystal with the zinc-blende structure. They examined the effect of changes in the positions of the surface atoms upon the energies of the surface states thereby illustrating the flexibility and power of the resolvent technique. Very recently, van der Avoird *et al.*,[31] have set up a numerical procedure based on the resolvent technique applied to a finite-slab geometry. This technique should be suitable for quantitative calculations on real systems, but results from this approach are yet to appear.

As we will see below, the resolvent technique requires knowledge of the bulk Green's function and the perturbation required to create the surface. The calculations presented above [22-31] result in a determination of the energy of the surface state as a function of wave vector parallel to the surface. The density of states is generally not obtained. A variation of the resolvent method was used by Kalkstein and Soven[32] wherein they solve directly for the Green's function appropriate for the surface. This allows them to calculate direct-

ly the density of states for each layer in the crystal. Thus, the effect of the surface on the bulk electronic levels can be directly seen independent of whether surface states exist. Bose and Foo[33] have recently performed a similar calculation on a one-dimensional binary system simulating an ionic crystal.

The phase-shift technique, coupled with the Green's-function method, is a convenient way to study the effect of a perturbation upon the energy levels of a general Hamiltonian. DeWitt[34] presented the essential elements of the phase-shift technique which has been formally applied to the problem of surfaces by Blandin[35] and Toulouse.[36] The method calculates the phase shift in the Bloch waves due to scattering from a perturbation (the surface). This phase shift gives the change in the energy levels due to the perturbation and thus can be related to the change in the density of states. This, in turn, can be related to several physical properties of interest regarding the surface.

This approach has been applied to several model systems. Allan,[37] and Allan and Lenglart[38,39] have extensively studied the clean-surface properties of a one-electron-band crystal of various structures (sc, fcc, bcc). They showed how the surface perturbation can give rise to surface states as well as how the bulk states are changed due to the surface, and, in addition, they found the change in the electronic specific heat due to the creation of the surface.

The phase-shift approach can also be used to study chemisorption. Recently, Einstein[40] has expanded earlier work of Einstein and Schrieffer[41] to study the changes in the density of states caused by chemisorption. This application of the phase-shift technique complements the Green's-function approach to chemisorption that has been discussed by Schrieffer[42] and Grimley and Pisani.[43]

The main advantage of the phase-shift technique is that it gives directly the change in the density of states. This information is important since it is directly applicable to photoemission and chemisorption. No other method gives this same information in such a straightforward manner. The main disadvantage to the phase-shift technique is its dependence on knowledge of the crystal Green's function. Usually, one must use numerical techniques for even the simplest of model cases. As a consequence, all of the work to date[37-41] has been confined to studying model one-band crystals. These results, then, have only been useful in understanding the surface properties of metals.

In this paper, we apply the phase-shift technique for the first time to a model two-band crystal. An important point is that we have been able to obtain the Green's function for the bulk in an analytic form. Thus, whereas some numerical work is required, the complete calculation is no more difficult than the previously considered one-band crystals. The results of this calculation, then, are useful in understanding the surface properties of semiconductors and insulators.

In Sec. II we derive the bulk properties of our model. This includes the bulk band structure as well as the bulk-crystal Green's functions. In Sec. III we discuss the phase-shift technique and present the perturbations appropriate for the surface. Here we consider three distinct cases; i.e., one which yields no surface states, one which results in Shockley surface states, and finally one which produces Tamm surface states. We show the change in the density of states due to the creation of the surface and determine the surface contribution to the specific heat for each case. In Sec. IV we obtain the surface Green's function for the case in which there are no surface states. This allows us to find the local density of states for each layer in the crystal. In Sec. V we summarize our results.

II. BULK GREEN'S FUNCTIONS

The one-electron Hamiltonian for the bulk crystal is given by

$$H_0 = \frac{p^2}{2m_e} + \sum_l \sum_\beta U(\vec{r} - \vec{x}(l\beta)), \tag{1}$$

where p is the electron momentum operator; m_e and $\vec{r}$ are the mass and position, respectively, of the electron; and $\vec{x}(l\beta)$ is the position of the βth-type basis atom in the lth unit cell of the crystal. We consider a crystal with the CsCl structure so that the index β takes on two values, 1 or 2, for the two types of atoms in the unit cell. The term U is the electron-ion core potential which is centered on each atom site. As is common in the LCAO formalism, electron-electron interactions are neglected.

The solution of the Schrödinger equation is assumed to be of the form

$$\psi(\vec{r}) = \sum_l \sum_\beta C_{l\beta} \Phi(\vec{r} - \vec{x}(l\beta)), \tag{2}$$

where $\Phi(\vec{r} - \vec{x}(l\beta))$ is an atomic-like orbital for a free atom centered on site $(l\beta)$. For this calculation, we assume one orbital for each atom in the crystal, and, whereas the specific form of the orbital is never needed, the orbital is assumed to be spherically symmetric (s-like).

Substituting Eq. (2) into the Schrödinger equation and using the TB approximation we obtain the following matrix equation:

$$\sum_{l}\sum_{\beta} H_0(l'\beta', l\beta)C_{l\beta} = EC_{l'\beta'}, \tag{3}$$

where

$$H_0(l'\beta', l\beta) \equiv \langle l'\beta' | H_0 | l\beta \rangle , \tag{4}$$

$$\langle l'\beta' | l\beta \rangle = \delta_{ll'}\delta_{\beta\beta'}, \tag{5}$$

and

$$|l\beta\rangle \equiv \Phi(\vec{r} - \vec{x}(l\beta)). \tag{6}$$

Within the limits of the TB approximation, the diagonal elements of the Hamiltonian matrix become the orbital energies of the free atoms, E_1 and E_2. Thus,

$$\langle l\beta | H_0 | l\beta \rangle = E_\beta, \quad \beta = 1, 2. \tag{7}$$

For the off-diagonal elements (also called hopping integrals), we have for nearest neighbors

$$\langle l1 | H_0 | l2 \rangle \equiv \gamma_1, \tag{8}$$

and for second neighbors

$$\langle l1 | H_0 | l+1\,1 \rangle \equiv \gamma_2^{(1)} = 0, \tag{9}$$

$$\langle l2 | H_0 | l+1\,2 \rangle \equiv \gamma_2^{(2)} \equiv \gamma_2. \tag{10}$$

There are two types of second-neighbor hopping integrals indicated by the superscript in Eqs. (9) and (10) because there are two types of second neighbors. Later in the calculation we are forced to set one of these hopping integrals to zero so that the bulk Green's function can be expressed in analytic form. In ionic crystals, the two components generally have different radii which implies that the two second-neighbor hopping integrals will have different values, and quite often one will be significantly greater than the other. This justifies our neglect of one of the second-neighbor hopping integrals.

In our calculation, all energy terms are expressed in units of γ_1. The parameters E_1, E_2, and γ_2 are taken as adjustable. Although approximate values can be obtained for these parameters by assuming a particular form for the orbitals and the potential, we feel that more specific choices than the general ones we have made would by no means change the qualitative nature of our results. The geometry and parameters of the problem are shown in Fig. 1. In all the results presented in this paper, we have chosen $E_1 = 2.0$ and $E_2 = -2.0$ in units of γ_1.

Using the standard approach,[44] we assume the wave function to be of the Bloch form by assuming the coefficients $C_{l\beta}$ to be

$$C_{l\beta} = N^{-1/2} w(\beta | \vec{k} j) e^{i\vec{k}\cdot\vec{x}(l)}, \quad j = 1, 2, \tag{11}$$

where $\vec{k}$ is the wave vector, j is the band index, and N is the number of unit cells in the crystal.

By substituting Eq. (11) into Eq. (3), and using the matrix element defined in Eqs. (7)–(10), we obtain a (2×2) secular matrix equation which can be solved to obtain the bulk energy bands. We find

$$\begin{aligned} E_{\vec{k}j} = {} & \tfrac{1}{2}(E_1 + E_2) + (\gamma_2^{(1)} + \gamma_2^{(2)}) f_2(\vec{\phi}) \\ & \pm \tfrac{1}{2}\{[E_1 - E_2 + 2(\gamma_2^{(1)} - \gamma_2^{(2)}) f_2(\vec{\phi})]^2 \\ & + 256\gamma_1^2 f_1^2(\vec{\phi})\}^{1/2}, \end{aligned} \tag{12}$$

where

$$f_1(\vec{\phi}) \equiv \cos\tfrac{1}{2}\phi_x \cos\tfrac{1}{2}\phi_y \cos\tfrac{1}{2}\phi_z, \tag{13}$$

$$f_2(\vec{\phi}) \equiv \cos\phi_x + \cos\phi_y + \cos\phi_z, \tag{14}$$

$$\vec{\phi} \equiv a_0\vec{k}, \tag{15}$$

and where a_0 is the crystal lattice spacing. In Eq. (12), the plus (minus) sign is associated with the branch index $j = 1$ (2).

In this paper we are concerned with the surface properties of the (001) surface (see Fig. 1). For this surface, the wave-vector components parallel to the surface (k_x and k_y) are good quantum numbers, but the wave vector perpendicular to the surface (k_z) is not. The Brillouin zone for the bulk crystal is a cube with sides of length $2\pi/a_0$. The Brillouin zone for the surface is a square with

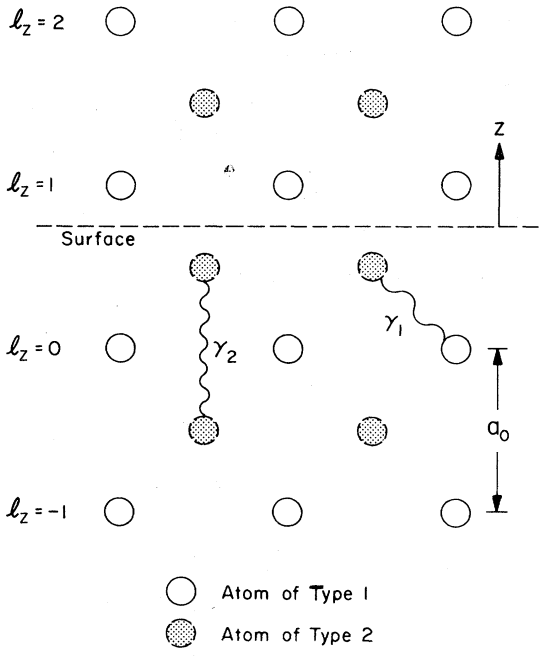

FIG. 1. Geometry of the (001) surface of a crystal with the CsCl structure. The plane of atoms of type 2 is a distance $\frac{1}{2}a_0$ behind the plane of atoms of type 1. The first-neighbor interaction is γ_1 and the second-neighbor interaction between atoms of type 2 is γ_2.

sides of length $2\pi/a_0$. To get the projection of the bulk energy bands onto the surface Brillouin zone, we sweep the z component of the wave vector k_z from the value 0 to π/a_0 (the energy expression is symmetric with respect to reflection of k_z so that only half of the k_z values are needed).

In Fig. 2 we present the results obtained for a segment of the surface Brillouin zone where we have chosen a particular value of k_y. The zero of energy is taken to be the average of the orbital energies of the free atoms. In Fig. 2(a) we show the energy bands for the case in which only the nearest-neighbor hopping integral is included. In Figs. 2(b) and 2(c), the second-neighbor interactions $\gamma_2^{(1)}$ and $\gamma_2^{(2)}$, respectively, are added to the first-neighbor calculation. We see that $\gamma_2^{(1)}$ affects

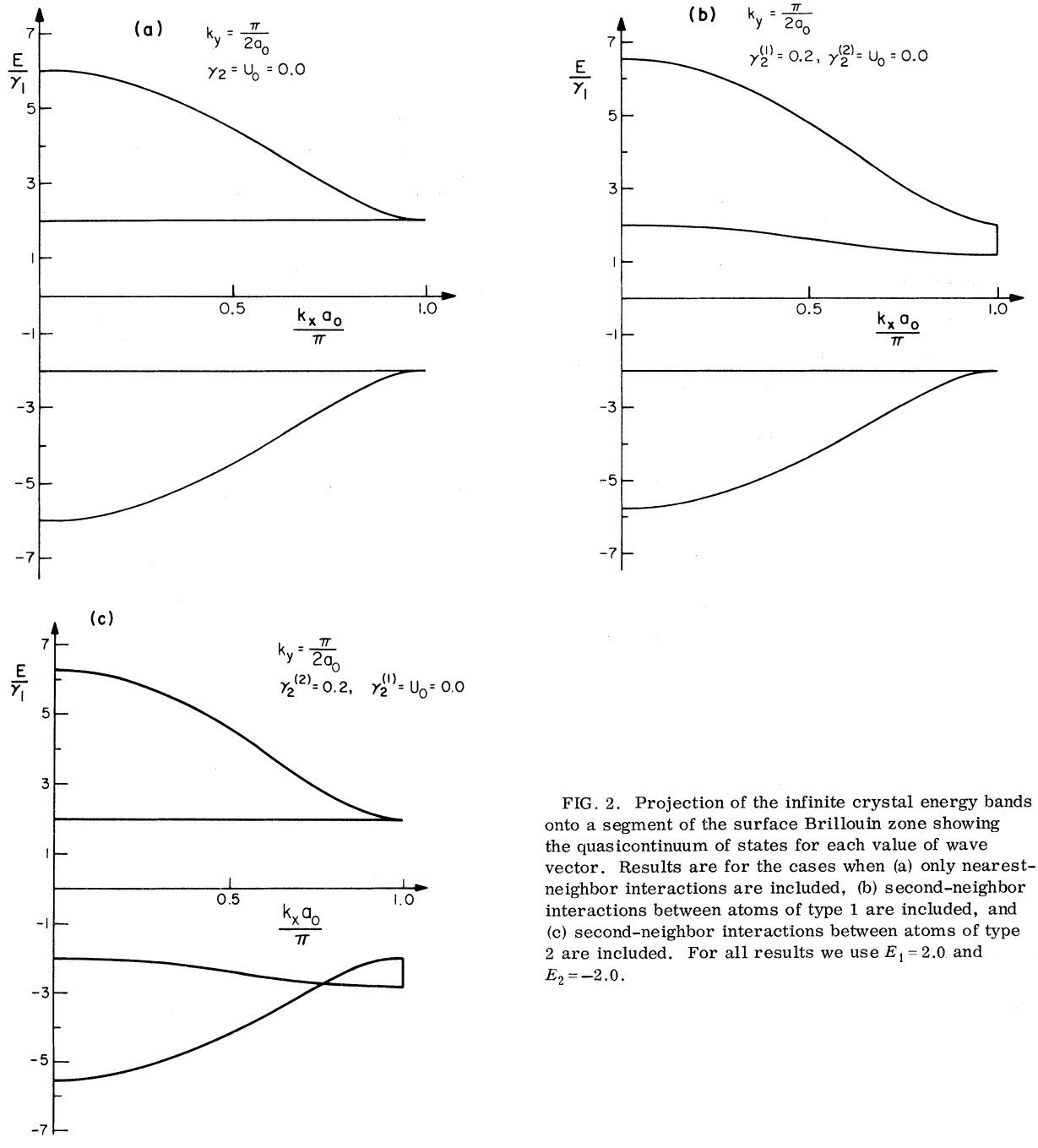

FIG. 2. Projection of the infinite crystal energy bands onto a segment of the surface Brillouin zone showing the quasicontinuum of states for each value of wave vector. Results are for the cases when (a) only nearest-neighbor interactions are included, (b) second-neighbor interactions between atoms of type 1 are included, and (c) second-neighbor interactions between atoms of type 2 are included. For all results we use $E_1 = 2.0$ and $E_2 = -2.0$.

the upper band and $\gamma_2^{(2)}$ affects the lower band. Since in a semiconductor only the lower band is filled, we have made the arbitrary choice of retaining $\gamma_2^{(2)} = \gamma_2$ in our calculations and setting $\gamma_2^{(1)} = 0$.

In order to determine the Green's function, we must know the eigenvector $w(\beta|\vec{k}j)$ of the (2×2) Hamiltonian matrix. From Eqs. (3) and (12), we obtain

$$w(1|\vec{k}j) = -Fe^{-i(\phi_x+\phi_y+\phi_z)/2}/\Delta\,, \tag{16}$$

$$w(2|\vec{k}j) = (E_1 - E_{\vec{k}j})/\Delta\,, \tag{17}$$

where

$$F \equiv 8\gamma_1 f_1(\vec{\phi})\,, \tag{18}$$

$$\Delta \equiv [F^2 + (E_1 - E_{\vec{k}j})^2]^{1/2}\,. \tag{19}$$

The retarded Green's function satisfies the following matrix equation[45]:

$$\sum_{l'}\sum_{\beta'}\left[H_0(l\beta, l'\beta') - (E + i\epsilon)\delta_{ll'}\delta_{\beta\beta'}\right] \times G^{(0)}(l'\beta', l''\beta'', E) = -\delta_{ll''}\delta_{\beta\beta''}\,, \tag{20}$$

where the superscript zero denotes the Green's function for the bulk crystal. The term $i\epsilon$, which is appropriate for a retarded Green's function, is a positive imaginary infinitesimal which will be dropped in the subsequent discussion until needed in Eq. (37). The Green's function can be related to the eigenvalues and eigenvectors of the Hamiltonian matrix by[46]

$$G^{(0)}(l\beta, l'\beta', E) = \frac{1}{N}\sum_{\vec{k}j}\frac{w(\beta|\vec{k}j)w^*(\beta'|\vec{k}j)}{E - E_{\vec{k}j}} \times e^{i\vec{k}\cdot\vec{x}(ll')}\,, \tag{21}$$

where

$$\vec{x}(ll') = \vec{x}(l) - \vec{x}(l')\,, \tag{22}$$

and the summation is over all wave vectors in the three-dimensional Brillouin zone and over the two branch indices. That Eq. (21) satisfies Eq. (20) can be seen by direct substitution. Performing explicitly the summation over j in Eq. (21) gives

$$G^{(0)}(l\beta, l'\beta', E) = \frac{1}{N}\sum_{\vec{k}}\left(\frac{w(\beta|\vec{k}1)w^*(\beta'|\vec{k}1)}{E - E_{\vec{k}1}} + \frac{w(\beta|\vec{k}2)w^*(\beta'|\vec{k}2)}{E - E_{\vec{k}2}}\right)e^{i\vec{k}\cdot\vec{x}(ll')}\,. \tag{23}$$

Substituting Eqs. (12), (16), and (17) into Eq. (23) gives for the bulk Green's functions

$$G^{(0)}(l1, l'1, E) = \sum_{\vec{k}}(E - E_B)D_B(ll')\,, \tag{24}$$

$$G^{(0)}(l2, l'2, E) = \sum_{\vec{k}}(E - E_1)D_B(ll')\,, \tag{25}$$

$$G^{(0)}(l1, l'2, E) = \sum_{\vec{k}}FD_B(ll')e^{-i(\phi_x+\phi_y+\phi_z)/2}\,, \tag{26}$$

$$G^{(0)}(l2, l'1, E) = \sum_{\vec{k}}FD_B(ll')e^{i(\phi_x+\phi_y+\phi_z)/2}\,, \tag{27}$$

where

$$D_B(ll') \equiv \frac{e^{i\vec{k}\cdot\vec{x}(ll')}}{N[(E - E_1)(E - E_B) - F^2]} \tag{28}$$

and

$$E_B \equiv E_2 + 2\gamma_2 f_2(\vec{\phi})\,. \tag{29}$$

An important feature of this calculation is the fact that, whereas Eq. (23) appears to be cumbersome, the eigenvalues and eigenvectors combine in just the right way to make the needed bulk Green's functions in Eqs. (24)–(27) rather simple.

In order to study the surface properties, it is appropriate to express the bulk Green's functions in a mixed Bloch-Wannier representation.[32,38,39] This effectively reduces the three-dimensional problem into a number of one-dimensional problems. As we will show below, each one-dimensional problem can be solved analytically. Thus, we exploit the translational symmetry parallel to the surface by expanding the bulk Green's functions in terms of $\vec{k}_s\ (\equiv \vec{\phi}_s/a_0)$, the wave vector parallel to the surface.

$$G^{(0)}(l\beta, l'\beta', E) = \frac{1}{N_s}\sum_{\vec{k}_s}G^{(0)}(l_z\beta, l_z'\beta', \vec{\phi}_s, E) \times e^{i\vec{k}_s\cdot\vec{x}(ll')}\,, \tag{30}$$

where N_s is the number of two-dimensional unit cells in the surface and l_z labels the unit cells in the direction perpendicular to the surface.

By comparing Eq. (30) with the results in Eqs. (24)–(27), the bulk Green's functions in the mixed representation become

$$G^{(0)}(l_z1, l_z'1, \vec{\phi}_s, E) = \sum_{k_z}(E - E_B)D_s(l_zl_z')\,, \tag{31}$$

$$G^{(0)}(l_z2, l_z'2, \vec{\phi}_s, E) = \sum_{k_z}(E - E_1)D_s(l_zl_z')\,, \tag{32}$$

$$G^{(0)}(l_z1, l_z'2, \vec{\phi}_s, E) = \sum_{k_z}FD_s(l_zl_z') \times e^{-i(\phi_x+\phi_y+\phi_z)/2}\,, \tag{33}$$

$$G^{(0)}(l_z2, l_z'1, \vec{\phi}_s, E) = \sum_{k_z}FD_s(l_zl_z') \times e^{i(\phi_x+\phi_y+\phi_z)/2}\,, \tag{34}$$

where

$$D_s(l_z l_z') \equiv \frac{e^{ik_z x (l_z l_z')}}{L_z[(E-E_1)(E-E_B)-F^2]}\ , \tag{35}$$

and where L_z is the number of unit cells in the z direction ($L_z N_s = N$).

To obtain the Green's functions in closed analytic form, we convert the sums to integrals through the transformation

$$\sum_{k_z} f(k_z) \to \frac{L_z}{2\pi}\int_{-\pi}^{\pi} d\phi_z f\left(\frac{\phi_z}{a_0}\right). \tag{36}$$

All of the resulting integrals are of the general form[47]

$$\int_{-\pi}^{\pi} d\phi_z \frac{\cos(l_z\phi_z)}{\cos\phi_z - \xi + i\epsilon} = \frac{4\pi t^{1+|l_z|}}{t^2-1}\ , \tag{37}$$

where

$$t = \begin{cases} \xi - (\xi^2-1)^{1/2}, & \xi > 1\ , \\ \xi + i(1-\xi^2)^{1/2}, & |\xi| < 1\ , \\ \xi + (\xi^2-1)^{1/2}, & \xi < -1\ . \end{cases} \tag{38}$$

It might be noted in passing that obtaining the integrals in the form of Eq. (37) is the step that forces us to set one of the second neighbor hopping integrals to zero.[48]

The final results for the bulk Green's functions are

$$G^{(0)}(l_z 1, l_z' 1, \vec{\phi}_s, E) = 2aPt^{|l_z - l_z'|+1} - 2\gamma_2 Pt[t^{|l_z - l_z'+1|} + t^{|l_z - l_z'-1|}], \tag{39}$$

$$G^{(0)}(l_z 2, l_z' 2, \vec{\phi}_s, E) = 2dPt^{|l_z - l_z'|+1}, \tag{40}$$

$$G^{(0)}(l_z 1, l_z' 2, \vec{\phi}_s, E) = 2fPt[t^{|l_z - l_z'|} + t^{|l_z - l_z'-1|}]e^{-i(\phi_x+\phi_y)/2}, \tag{41}$$

$$G^{(0)}(l_z 2, l_z' 1, \vec{\phi}_s, E) = 2fPt[t^{|l_z - l_z'|} + t^{|l_z - l_z'+1|}]e^{i(\phi_x+\phi_y)/2}, \tag{42}$$

where

$$a \equiv E - E_2 - 2\gamma_2(\cos\phi_x + \cos\phi_y), \tag{43}$$

$$P \equiv 1/B(t^2-1), \tag{44}$$

$$d \equiv E - E_1, \tag{45}$$

$$f \equiv 4\gamma_1 \cos(\tfrac{1}{2}\phi_x)\cos(\tfrac{1}{2}\phi_y), \tag{46}$$

$$\xi \equiv -A/B, \tag{47}$$

$$A \equiv ad - 2f^2, \tag{48}$$

$$B \equiv -2\gamma_2 d - 2f^2. \tag{49}$$

Two important properties of the Green's functions are apparent from these equations. First, in the bulk, the Green's functions depend only upon the separation distance between layers, $l_z - l_z'$, and not on the value of l_z and l_z' separately. Second, the two Green's functions in Eqs. (39) and (40) are complex only when the magnitude of the parameter ξ is less than unity [see Eq. (38)]. This occurs only when the energy E falls within one of the two bands [see Eqs. (43)–(49)].

Except for an ambiguity in sign which is fully discussed in both Sec. IV and in the Appendix, the set of equations from Eq. (38)–(49) completely defines the bulk Green's functions. It requires only a simple numerical program to obtain any of the bulk Green's functions for arbitrary energy E and two-dimensional wave vector $\vec{\phi}_s$.

III. PHASE-SHIFT CALCULATIONS

We form the (001) surface by passing an imaginary plane between atoms of type 2 in the $l_z = 0$ plane and atoms of type 1 in the $l_z = 1$ plane as shown in Fig. 1. Each surface formed consists of only one type of atom. The effects of the surface formation can be introduced into the Hamiltonian by adding a perturbation term which exactly cancels all interactions which occur across the imaginary plane. Thus, in matrix notation analogous to Eq. (4), we write for the perturbed system

$$H(l\beta, l'\beta') = H_0(l\beta, l'\beta') + V(l\beta, l'\beta'), \tag{50}$$

where V is the surface perturbation term. If, for example, we consider the bulk crystal to have only nearest-neighbor interactions (i.e., $\gamma_2 = 0$), then the perturbation term is

$$V(l\beta, l'\beta') = -\gamma_1(\delta_{l_z 1}\delta_{\beta 1}\delta_{l_z' 0}\delta_{\beta' 2} + \delta_{l_z 0}\delta_{\beta 2}\delta_{l_z' 1}\delta_{\beta' 1}) \times (\delta_{l_x l_x'}\delta_{l_y l_y'} + \delta_{l_x l_x'}\delta_{l_y l_y'+1} + \delta_{l_x l_x'+1}\delta_{l_y l_y'} + \delta_{l_x l_x'+1}\delta_{l_y l_y'+1}). \tag{51}$$

In the resolvent technique,[25-27] the energy of the surface state is obtained from the determinant equation

$$\det\left(\delta_{ll'}\delta_{\beta\beta'} - \sum_{l''}\sum_{\beta''} V(l\beta, l''\beta'') \times G^{(0)}(l''\beta'', l'\beta', E)\right) = 0. \tag{52}$$

The value of E for which this equation is satisfied is the surface state energy. The equation is valid only for energies outside the bands where the Green's functions are real. For energies inside the band, the real part of Eq. (52) gives resonances inside the bulk bands. The matrices appearing in Eq. (52) are infinite in size. Since the translational symmetry in the direction parallel to the

surface is preserved in the cleaved crystal, each matrix in Eq. (52) can be expressed in the mixed Bloch-Wannier representation. For the Green's function, this is done in Eq. (30). For the perturbation matrix, we have

$$V(l_z\beta, l_z'\beta', \vec{\phi}_s) = \sum_{l_x, l_y} V(l_x\, l_y\, l_z\beta, 00 l_z'\beta') \times e^{-i\vec{k}_s\cdot\vec{x}(11')} . \quad (53)$$

In contrast to the matrix in Eq. (51), the nonzero elements in Eq. (53) form a matrix which is finite in size; in fact, it is quite small, either (2×2) or (3×3) in this paper.

In analogy with the resolvent technique, the phase shift technique[37-39] defines the determinant function (Fredholm determinant)

$$D(\vec{\phi}_s, E) = \det\left(\delta_{l_z l_z'}\delta_{\beta\beta'} - \sum_{l_z''}\sum_{\beta''} V(l_z\beta, l_z''\beta'', \vec{\phi}_s) \times G^{(0)}(l_z''\beta'', l_z'\beta', \vec{\phi}_s, E)\right). \quad (54)$$

For energies E outside the bands, the condition

$$D(\vec{\phi}_s, E) = 0 \quad (55)$$

gives the energy of the surface state for each value of $\vec{\phi}_s$. For energies inside the bands, the function $D(\vec{\phi}_s, E)$ is complex. For this case, we define the partial phase-shift function

$$\eta(\vec{\phi}_s, E) = -\arg D(\vec{\phi}_s, E) . \quad (56)$$

The total phase shift per surface unit cell is obtained by summing the partial phase shift over the surface Brillouin zone, i.e.,

$$\eta(E) = \frac{1}{N_s}\sum_{\vec{\phi}_s} \eta(\vec{\phi}_s, E) . \quad (57)$$

It is related in a simple way to the change in the density of states. We have[35,36]

$$\Delta n(E) = \frac{1}{\pi}\frac{d\eta(E)}{dE} , \quad (58)$$

where $\Delta n(E)$ is the shift in the number of energy states per unit energy per surface unit cell. This change in the density of states is the desired result of this portion of the calculation. From it, several physical properties of the surface can be determined.

To proceed with this calculation, then, we must define the explicit form of the perturbation matrix which creates the surface. In this paper we consider three different model cases. For *model I*, we consider the bulk crystal to have only nearest-neighbor interactions. To create the surface we cancel the effect of the transfer integrals across the imaginary plane. Thus, the perturbation for model I is given in Eq. (51). Upon substitution into Eq. (53), we obtain a matrix whose nonzero elements can be put into (2×2) form

$$V(l_z\beta, l_z'\beta', \vec{\phi}_s) = \begin{bmatrix} 0 & -f\chi(\vec{\phi}_s) \\ -f\chi^*(\vec{\phi}_s) & 0 \end{bmatrix} , \quad (59)$$

where

$$\chi(\vec{\phi}_s) = e^{i(\phi_x+\phi_y)/2} , \quad (60)$$

and where f is given in Eq. (46). The rows and columns of this matrix are labeled by the rows of atoms in Fig. 1 that participate in the perturbation. For this case, the first row indicates a value of $(l_z\beta) = (02)$ while the second row is for $(l_z\beta) = (11)$. For all other values of $(l_z\beta)$, the matrix elements of V are identically zero. Thus, whereas matrix V is technically infinite in size, there are only two nonzero terms. As we will see below, there are no surface states for model I.

For *model II* we consider the bulk crystal to have both first and second neighbor interactions as shown in Fig. 1 and discussed in Sec. II. For this case the perturbation needed to create the surface extends to the second layer from the surface, and the resulting perturbation matrix is (3×3). We have

$$V(l_z\beta, l_z'\beta', \vec{\phi}_s) = \begin{bmatrix} 0 & -f\chi(\vec{\phi}_s) & -\gamma_2 \\ -f\chi^*(\vec{\phi}_s) & 0 & 0 \\ -\gamma_2 & 0 & 0 \end{bmatrix} . \quad (61)$$

For this matrix, the third row and column are labeled by the atomic row $(l_z\beta) = (12)$. As we will see below, model II gives rise to Shockley surface states.

For *model III* we again consider the situation in model I where only first-neighbor interactions are assumed. However, upon creating the surface we assume that the orbital energy on the first layer of atoms on each surface is changed by an amount U_0. The physical basis for this perturbation is that the crystal potential at the surface is different from its value in the bulk. The perturbation matrix for this case is

$$V(l_z\beta, l_z'\beta', \vec{\phi}_s) = \begin{bmatrix} U_0 & -f\chi(\vec{\phi}_s) \\ -f\chi^*(\vec{\phi}_s) & U_0 \end{bmatrix} , \quad (62)$$

where the labels of the rows and columns are the same as in model I. The reason for considering this model is that it results in Tamm surface states.

The surface states which fall outside of the bands

can now be easily determined by the resolvent technique. We have numerically calculated the Fredholm determinant [Eq. (54)] for each of the three models as a function of energy E for various choices of wave vector $\vec{\phi}_s$. When the determinant goes through zero as we vary E, we have a surface state. For model I, this never occurs which means there are no surface states within the context of this model.

For model II, Shockley surface states occur in the band gap. In Fig. 3 we show a three-dimensional view of the energy band structure for one-quarter of the surface Brillouin zone. The shaded region just above the valence band is the Shockley surface state band. In Fig. 4 we show a detail of this surface state band as a function of ϕ_x for a particular choice of ϕ_y. The energy between the crossing point in the bulk band and the surface state curve is exactly equal to the magnitude of γ_2, which for the calculations in this paper has been chosen to be 0.2, in units of γ_1. Note that the surface state band merges with the bulk band and stops at a point in the Brillouin zone slightly beyond the position where the top and bottom of the valence band cross. This property of the surface state band is shown fully in Fig. 5 where we plot the boundary of the surface state inside the two-dimensional surface Brillouin zone.

Finally, in Fig. 6 we show the Tamm surface states which arise from model III. Here, surface states exist above both the valence band and the conduction band (note break in energy axis). The surface state above the conduction band merges with the bulk band near the Brillouin-zone boundary. At the Brillouin-zone boundary, the energy difference between the band edges and the surface states is equal to the perturbation U_0 which for

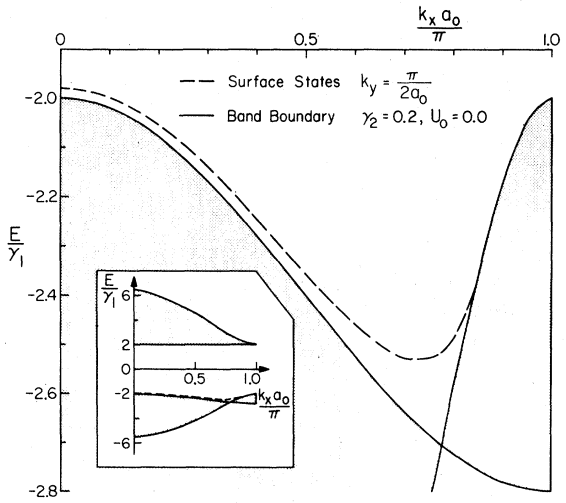

FIG. 4. Detail of the surface states for model II for a particular segment, $k_y = \pi/2a_0$, of the surface Brillouin zone.

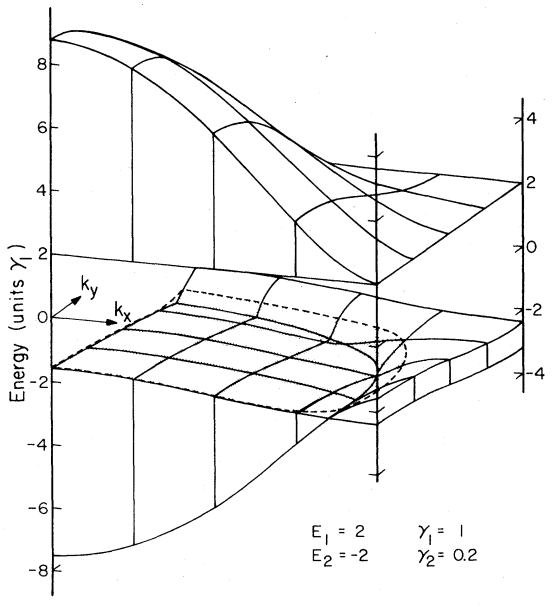

FIG. 3. Energy bands for one-quarter of the surface Brillouin zone for model II showing the Shockley surface states (shaded area) lying just above the valence band.

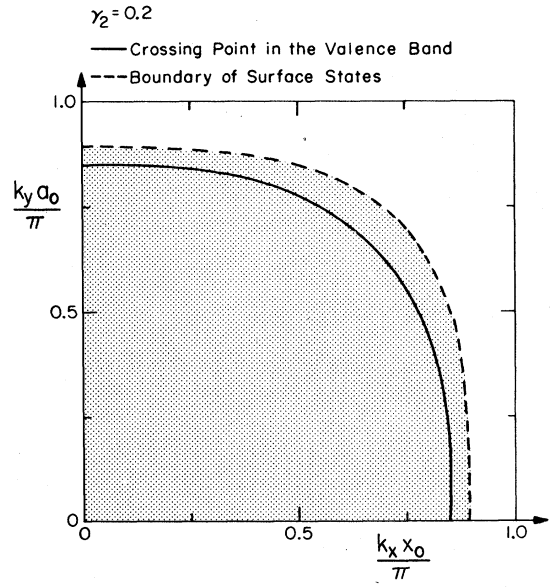

FIG. 5. Shaded region shows the region in the surface Brillouin zone for which Shockley surface states exist in model II.

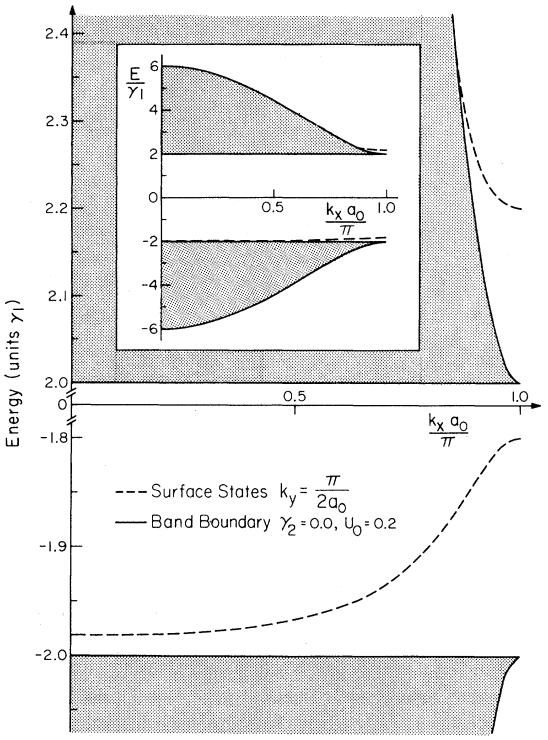

FIG. 6. Position of the Tamm surface states for model III for a particular segment, $k_y = \pi/2a_0$, of the surface Brillouin zone. Note the break in the vertical scale.

these calculations has been chosen to be 0.2 in units of γ_1.

It is important to note a significant difference in the existence conditions for the surface states in the present calculation compared with previous results. In this work, Shockley surface states appear in model II for arbitrarily small values of γ_2 and Tamm surface states appear in model III for arbitrarily small values of U_0. In the one-band model calculations of Allan and Lenglart[38,39] only Tamm states appear and only when the surface perturbation U_0 exceeds a certain critical value [for the (001) surface of simple cubic crystals, the existence condition is that $U_0 > \gamma_1$]. It is also generally true for one-dimensional systems (as discussed in Sec. I) that a perturbation exceeding a critical value is needed before surface states appear.

States in the bulk bands are localized on one of the two types of atoms in the crystal. States with energies in the upper (conduction) band are localized on atoms of type 1, whereas states with energies in the lower (valence) band are localized on atoms of type 2. This is because we chose E_1 to be positive and E_2 to be negative. Concerning surface states, then, those which originate from the upper band (the upper surface state for model III) are localized on the surface where the first layer consists of atoms of type 1 (upper surface in Fig. 1). On the other hand, surface states originating from the lower band (model II and lower state in model III) are localized on the surface where the first layer of atoms is of type 2 (lower surface in Fig. 1).

For arbitrary wave vector $\vec{\phi}_s$, the Fredholm determinant [Eq. (54)] can also be evaluated for energies inside the bands for each of the three models. In this case the determinant is complex, and by using Eq. (56) the partial phase shift can be calculated. By way of illustration, in Fig. 7 we have plotted the partial phase shift for a particular point in the surface Brillouin zone. In Fig. 7(a) we show the partial phase shift for model I at the point $\phi_x = \phi_y = \frac{1}{2}\pi$. Since there are no surface states in this model, the phase shift is nonzero only for energies inside the bands [compare with Fig. 2(a)]. The phase-shift function is antisymmetric with respect to the energy zero due to the sign of the Green's function as is fully discussed in Sec. IV and the Appendix.

In Fig. 7(b) we show the partial phase shift for model II. In this figure the surface state which exists just above the valence band is indicated by the step in the partial phase shift from the value $-\pi$ to 0. As we move down in energy from the energy zero, the phase shift jumps from 0 to $-\pi$ at the zero of the Fredholm determinant.[34,49] It stays constant at $-\pi$ until the top of the valence band is reached at which point it jumps to $-\frac{1}{2}\pi$. The results for model III are presented in Fig. 7(c). Again we see the effect of the surface state just above the valence band. In Fig. 7(d) we show the partial phase shift for model III, but this time for a different wave-vector point which is closer to the zone boundary where the bands are more narrow (note the change in scale). Here we see the effect of the two surface states, one above the valence band and one above the conduction band.

Superficially, there seem to be discrepancies between our partial phase shifts and those obtained previously for one-band crystals by Allen and Lenglart.[39] They find a jump of $\pm 2\pi$ at the surface-state energies rather than $-\pi$ as in our case. The difference is explained by realizing that when a crystal is cleaved, *two* surfaces are formed. The properties derived from the phase shift technique are the combined contributions from *both* surfaces. In the model of Allan and Lenglart,[39] the two created surfaces are identical since their model contains only one type of atom. Thus, if surface states exist (in their model only Tamm surface states are possible), they exist on both

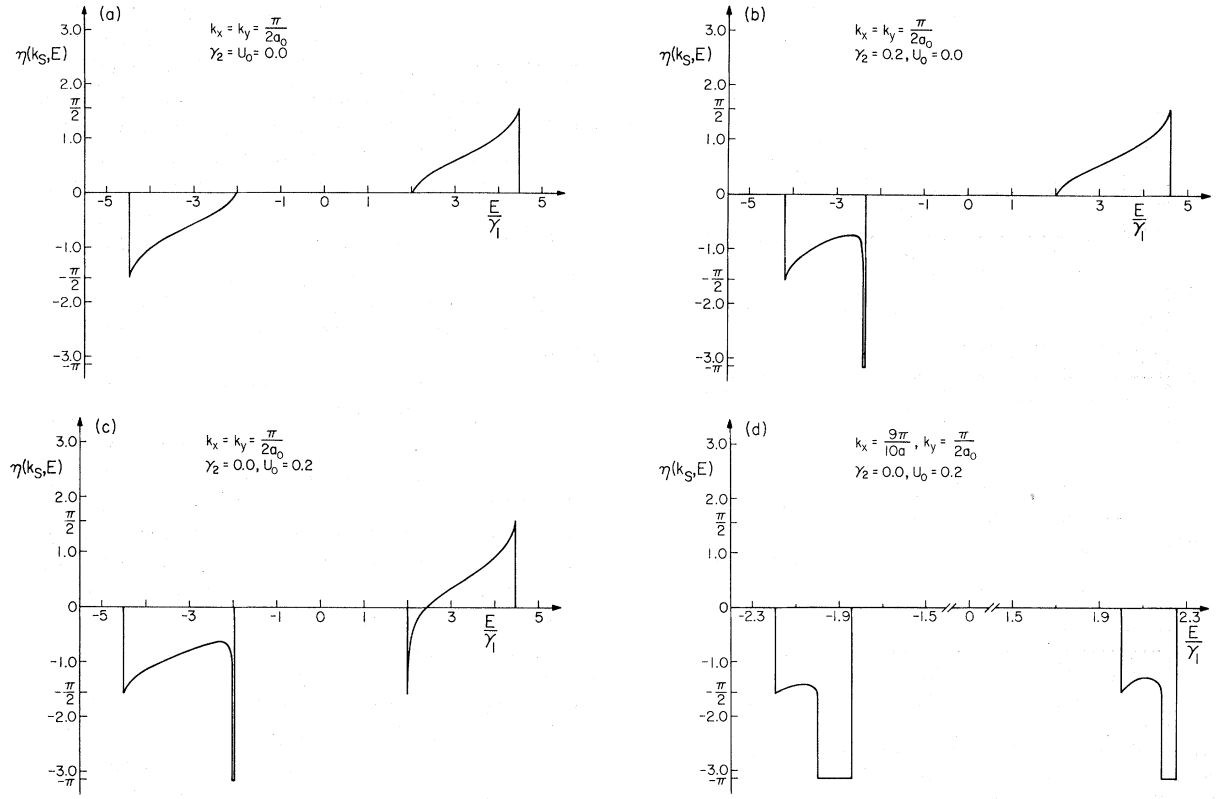

FIG. 7. Partial phase shift as a function of energy for a particular point, $k_x = k_y = \pi/2a_0$, in the surface Brillouin zone for (a) model I, (b) model II, and (c) model III. (d) The partial phase shift at a point near the zone edge, $k_x = 9\pi/10a_0$ and $k_y = \pi/2a_0$, for model III. Note the break in scale.

surfaces resulting in a phase shift of $\pm 2\pi$. (The plus or minus sign distinguishes between states appearing below or above the single energy band, respectively.) In our calculation, however, the two surfaces formed are not identical (see Fig. 1). The surface states are localized on either one or the other of the surfaces. Therefore, our phase shift changes by $-\pi$, with the minus sign due to the fact the surface state appears above the band from which it originates. If we had cleaved the CsCl crystal along the (110) plane, the two surfaces formed would be identical and the phase shift would then jump by $\pm 2\pi$ at the surface state energy.

To obtain the total phase shift function, the partial phase shift function for each wave vector must be summed over the surface Brillouin zone as shown in Eq. (57). We have done this numerically by choosing a uniform displaced mesh of points in the irreducible segment of the Brillouin zone. The method of deriving this mesh, which is the optimum set of points of a given size for accurately determining averages over the Brillouin zone, has been fully described recently by Cunningham.[50] If the number of points chosen is too small, the results of the summation will fluctuate as the number of points is changed. We have increased the number of points in the sample until the fluctuations in the results have become small. Typically, this means that we used samples containing 400 points.

The total phase shifts for the three models are shown in Fig. 8. For model I we obtain the simple antisymmetric curve shown in Fig. 8(a). The curves start and stop at the bulk crystal band edges since there are no surface states. In Fig. 8(b) we show the total phase shift for model II. Since the inclusion of γ_2 does not change the shape of the conduction band and does not introduce surface states near that band, the total phase shift in the energy range $E > 0$ is very nearly the same as in Fig. 8(a). The results in the region of the valence band, however, are quite different due to the difference in the band shape and the presence of the surface state. Even though the partial phase shifts equal $-\pi$ between the bulk and surface states, the total phase shift does not reach the value of $-\pi$. This is due to the fact that there is not a single value of energy E which lies between

the bulk and surface state for every point in the Brillouin zone (see Figs. 3 and 4). The total phase shift for model III is shown in Fig. 8(c). Here, the total phase shift does reach a value of $-\pi$ since energies just above the valence band edge are always between the bulk and surface states for all points in the Brillouin zone (see Fig. 6). In addition, the presence of the surface state associated with the conduction band changes the total phase shift in the region of positive energies.

The interest in the total phase shift is due to the simple relation between it and the change in the density of states due to the creation of the surface [see Eq. (58)]. Upon taking the derivative of the curves in Fig. 8, we obtain the change in the density of states for each model, and these results are shown in Fig. 9. In Fig. 9(a) we show the

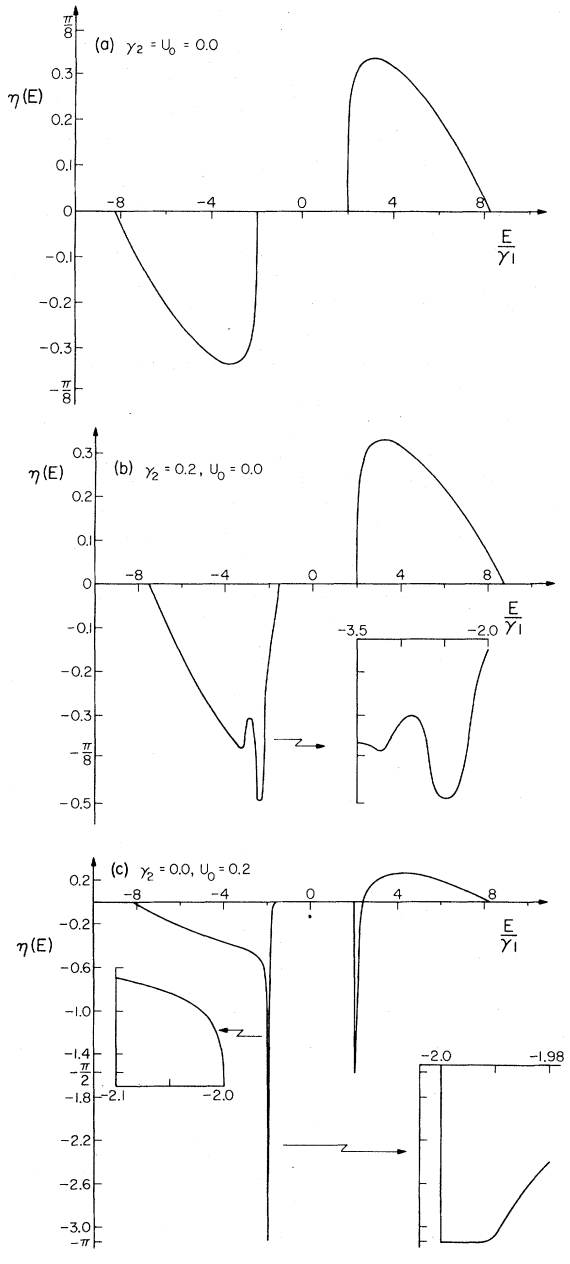

FIG. 8. Total phase shift as a function of energy for (a) model I, (b) model II, and (c) model III.

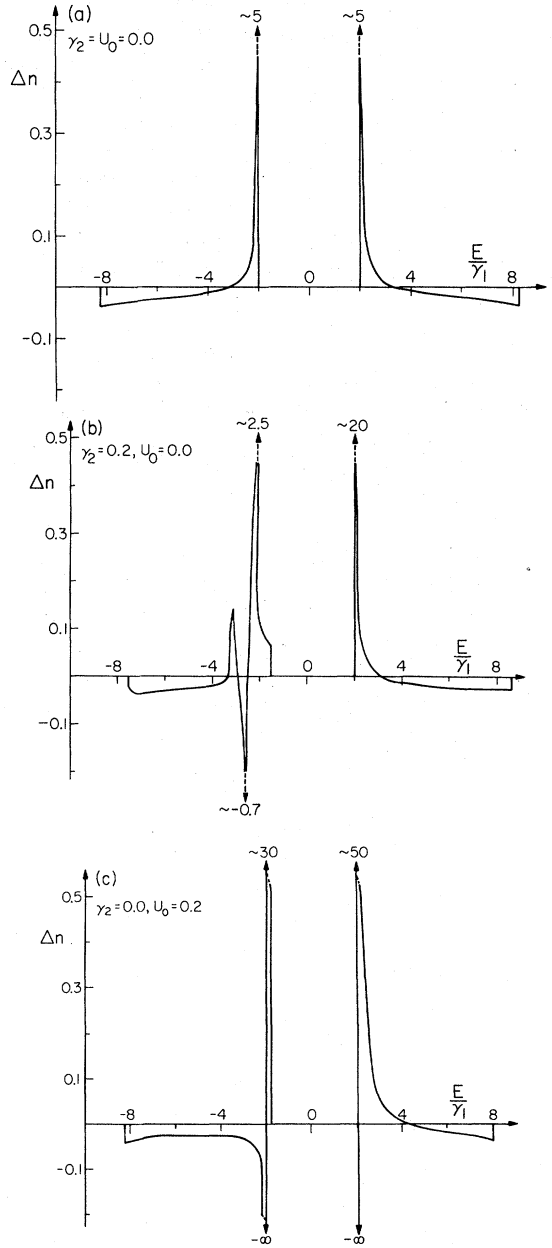

FIG. 9. Change due to the creation of the surface in the total density of states (per unit energy) per surface unit cell as a function of energy for (a) model I, (b) model II, and (c) model III.

results for model I. We see that the creation of the surface has shifted the bulk states toward the band gap by increasing the number of states near the gap and depleting the number of states far from the gap. The magnitude of the sharp peaks at the band edges is only approximate since the differentiation is done numerically, and small uncertainties in the phase shift values lead to large uncertainties in the derivative when the derivative is large.

In Fig. 9(b) we present the results for model II. The conduction band results are similar to the results in Fig. 9(a). The presence of the Shockley surface states, however, greatly changes the valence band results. The complexity of the changes in the density of states is a result of the band structure. The increase in the density of states at $E = -2.0$ is due to the presence of surface states. The increase in the density of states at $E = -3.2$ is analogous to the shift of bulk states toward the band gap in Fig. 9(a). The minimum in the density of states at $E = -2.8$ is due to the fact that more bulk states are removed in this region than there are surface states added.

In Fig. 9(c) we present the change in the density of states for model III. Here the interpretation is a little easier since the band structure is simpler. For the valence band, there is a sharp depletion of bulk states right at the band edge with all of the states being put into the surface states just inside the band gap. For the conduction band, again the bulk states are depleted right at the band edge, but this time the surface states have energies that overlap those of the bulk bands.

Once the change in the density of states is known, changes in the thermodynamic properties of the crystal due to the surface can be obtained. For example, the change in the electronic specific heat $\Delta C_v(T)$ is given by

$$\Delta C_v(T) = \int_{-\infty}^{\infty} dE\, E \Delta n(E) \frac{\partial f(E, T)}{\partial T} , \tag{63}$$

where $f(E, T)$ is the Fermi-Dirac function given by

$$f(E, T) = (e^{(E-\mu)/k_B T} + 1)^{-1} , \tag{64}$$

and where μ is the Fermi energy. We assume the Fermi energy to be exactly in the middle of the band gap ($\mu = 0$) and to be independent of temperature T. Another thermodynamic property, the surface entropy, is given by an integration of Eq. (63),

$$S_e(T) = \int_0^T \Delta C_v(T') \frac{dT'}{T'} . \tag{65}$$

In Fig. 10 we present the change in the electronic specific heat due to the surface for each of the three models. Three features are worth noting. First, the results for the three models are quite similar. This is expected since the addition of a weak second-neighbor interaction ($\gamma_2 = 0.2\gamma_1$) or a weak surface-atom perturbation ($U_0 = 0.2\gamma_1$) should not greatly change the thermodynamic properties. This is true even though two of the models have surface states, while one does not. Second, at low temperatures we find that the change in the specific heat approaches zero exponentially with temperature. This is consistent with the fact that the models have a forbidden energy gap in the change in the density of states. In contrast to this, we have also plotted in Fig. 10 the results obtained by Allan and Lenglart[38] for the (001) surface of a half-filled one-band simple cubic crystal. In this case, the change in the electronic specific heat at low temperature approaches zero linearly with temperature. Third, at high temperatures (possibly above the melting temperature of real crystals), the change in the specific heat becomes negative. This occurs because at high temperatures the levels far from the Fermi energy are more strongly weighted in the integral [Eq. (63)] than those close to the Fermi energy, and the change in the density of states for these levels (see Fig. 9) is negative.

In Fig. 11 we show the electronic surface entropy obtained from Eq. (65) for each of the three models. Again we see the exponential behavior at low temperatures. In addition, we see that the electronic surface entropy is positive for all temperatures as it should be.

A comment should be made regarding the positioning of the Fermi level. Since our method of creating the surface does not change the total number of electrons in the crystal, then the integral up to the Fermi level of the change in the density of states must vanish. From Eq. (58), this integral is proportional to the phase-shift function at the Fermi level. Thus, to insure that we conserve the number of electrons in the crystal, we have the condition

$$\eta(\mu) = \pi \int_{-\infty}^{\mu} \Delta n(E)\, dE = 0 . \tag{66}$$

This is one of the ways to express the Friedel[51] sum rule for perturbed systems. By examining Fig. 8, we see that without further changes, this condition forces us to place the Fermi level either inside the band gap or outside of the bands for all three models (for model III, we can also chose the Fermi level to be just above the conduction-band edge). Thus our model calculations are particularly suited for discussion of semiconductor or insulator properties. In order to apply our model to two-band metals, we would need to add

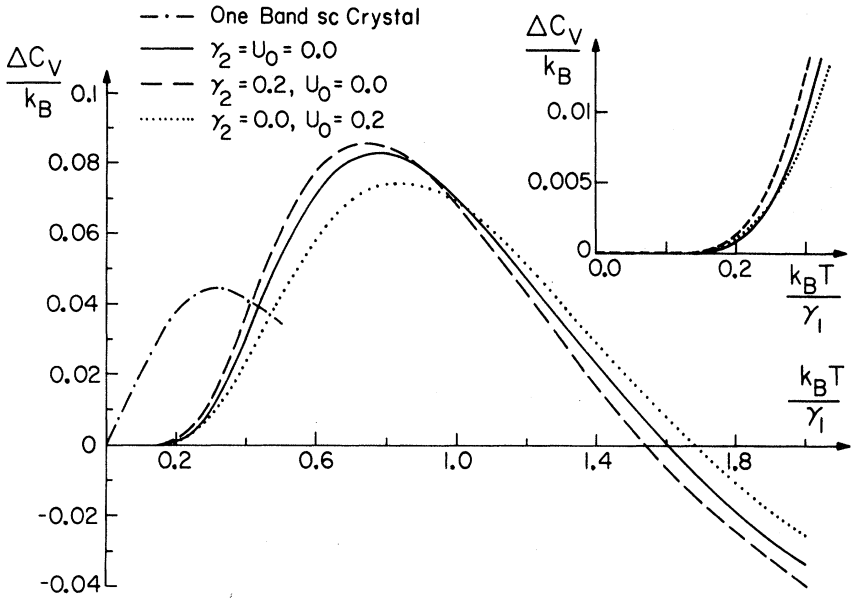

FIG. 10. Change due to the creation of the surface in the electronic specific heat as a function of temperature for each of the three models. The results for the half-filled one-band crystal (Ref. 38) are plotted for comparison.

a "self-consistency" term to the perturbation matrix in the same manner as Allan.[37]

IV. SURFACE GREEN'S FUNCTIONS

In this section we derive the Green's functions appropriate for the surface. There are two main reasons for doing this. First, the layer density of states can be calculated in the manner shown by Kalkstein and Soven.[32] This allows us to see directly how the effect on the electronic levels due to the surface perturbation is localized within the first few layers of the solid. From this we can make contact with photoemission experiments since it is the density of states near the surface that is measured, and this need not be the same as the density of states in the bulk. Second, the surface Green's functions can be used as a starting point in studying further changes in the crystal surface. Specifically, the surface Green's function can be used to study the effects of reconstruction[1,52] and chemisorption.[1,40-43]

In analogy with Eq. (20), the retarded surface

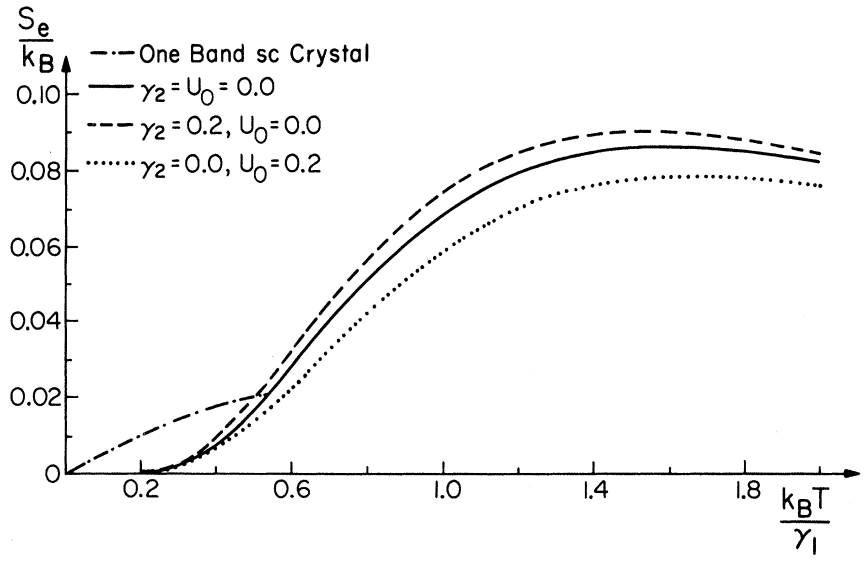

FIG. 11. Electronic contribution to the surface entropy as a function of temperature for each of the three models. The results for the half-filled one-band crystal (Ref. 38) are plotted for comparison.

Green's function satisfies the equation

$$\sum_{l'}\sum_{\beta'}[H(l\beta, l'\beta') - (E+i\epsilon)\delta_{ll'}\delta_{\beta\beta'}] \times G(l'\beta', l''\beta'', E) = -\delta_{ll''}\delta_{\beta\beta''} , \quad (67)$$

where H is given by Eq. (50), and where we have dropped the superscript (0) to represent the surface Green's function. By multiplying Eq. (67) by the bulk Green's function $G^{(0)}(l'''\beta''', l\beta)$ and by summing over indices l and β, we obtain

$$G(l'''\beta''', l''\beta'', E) = G^{(0)}(l'''\beta''', l''\beta'', E) + \sum_{l,\beta}\sum_{l',\beta'} G^{(0)}(l'''\beta''', l\beta, E) \times V(l\beta, l'\beta')G(l'\beta', l''\beta'', E) , \quad (68)$$

where V is the perturbation matrix given by Eq. (51). As in Eqs. (30) and (53), we convert the surface Green's function to the mixed Bloch-Wannier representation

$$G(l\beta, l'\beta', E) = \frac{1}{N_s}\sum_{\vec{k}_s} G(l_z\beta, l'_z\beta', \vec{\phi}_s, E) \times e^{i\vec{k}_s\cdot\vec{x}(ll')} . \quad (69)$$

In this representation, Eq. (68) becomes

$$G(l'''_z\beta''', l''_z\beta'', \vec{\phi}_s) = G^{(0)}(l'''_z\beta''', l''_z\beta'', \vec{\phi}_s) + \sum_{l_z\beta}\sum_{l'_z\beta'} G^{(0)}(l'''_z\beta''', l_z\beta, \vec{\phi}_s) \times V(l_z\beta, l'_z\beta', \vec{\phi}_s) \times G(l'_z\beta', l''_z\beta'', \vec{\phi}_s) , \quad (70)$$

where we have dropped the explicit dependence on E for convenience.

In this portion of the problem, we choose (for convenience) to consider only model I. Because of the particularly simple form of the perturbation matrix, Eq. (59), we can explicitly carry out the matrix multiplication in Eq. (70). In addition, we use the fact that $G(l_z\beta, l'_z\beta')$ is nonzero only if l_z and l'_z are on the same side of the surface. Thus, if we consider first the upper surface in Fig. 1, we obtain

$$G(l'_z\beta', l_z\beta) = G^{(0)}(l'_z\beta', l_z\beta) + G^{(0)}(l'_z\beta', 02)V(02, 11)G(11, l_z\beta) , \quad (71)$$

where we have suppressed the dependence on $\vec{\phi}_s$. By setting $l'_z = 1$ and $\beta' = 1$, we solve Eq. (71) for the surface Green's function to get

$$G(11, l_z\beta) = G^{(0)}(11, l_z\beta)/[1 - G^{(0)}(11, 02)V(02, 11)] . \quad (72)$$

Finally, this expression can be substituted back into Eq. (71) to give the general surface Green's functions. By substituting the explicit expressions in Eqs. (39)–(42) for the bulk Green's functions and after considerable algebraic manipulation, the surface Green's functions can be written (remember that l_z and $l'_z \geq 1$)

$$G(l_z\beta, l'_z1) = G^{(0)}(l_z\beta, l'_z1) - G^{(0)}(l_z + l'_z\beta, 11) , \quad (73)$$

$$G(l_z\beta, l'_z2) = G^{(0)}(l_z\beta, l'_z2) - G^{(0)}(l_z + l'_z\beta, 02) , \quad (74)$$

where $\beta = 1, 2$. Similarly, for the lower surface in Fig. 1 (l_z and $l'_z \leq 0$) we obtain

$$G(l_z\beta, l'_z1) = G^{(0)}(l_z\beta, l'_z1) - G^{(0)}(l_z + l'_z - 1\beta, 11) , \quad (75)$$

$$G(l_z\beta, l'_z2) = G^{(0)}(l_z\beta, l'_z2) - G^{(0)}(l_z + l'_z - 1\beta, 02) , \quad (76)$$

where $\beta = 1, 2$. The fact that the surface Green's function can be expressed as the difference of two bulk Green's functions is a significant simplification in our problem. This fact was recognized to be true for the one-band crystal surfaces by Dobrzynski and Mills,[52] and it is also true for a finite diatomic chain.[53]

The density of states on the layer labeled by l_z and β is related to the imaginary part of the surface Green's function by[32]

$$\rho(l_z\beta, E) = \frac{-1}{\pi N_s}\,\mathrm{Im}\sum_{\vec{\phi}_s} G(l_z\beta, l_z\beta, \vec{\phi}_s, E) . \quad (77)$$

Only the diagonal elements of the Green's-function matrix are needed. By substituting the analytic expressions for the bulk Green's functions into Eqs. (73)–(76), we obtain the simple expressions

$$G(l_z1, l_z1) = Jd(1 - t^{2l_z-1}), \quad l_z \geq 1 , \quad (78)$$

$$G(l_z2, l_z2) = Ja(1 - t^{2l_z}), \quad l_z \geq 1 , \quad (79)$$

$$G(l_z1, l_z1) = Jd(1 - t^{-2l_z+2}), \quad l_z \leq 0 , \quad (80)$$

$$G(l_z2, l_z2) = Ja(1 - t^{-2l_z+1}), \quad l_z \leq 0 , \quad (81)$$

where

$$J = 2t/B(t^2 - 1) , \quad (82)$$

and $\mathrm{Im}t$ is to be interpreted as $-\mathrm{sgn}(E)\mathrm{Im}t$, where $\mathrm{sgn}(E)$ is the sign of E.

The term $\mathrm{sgn}(E)$ is added because of an ambiguity in sign in taking the square root of a square. This ambiguity arises in all aspects of the use of this Green's function. The ambiguity is removed by comparing the results of the calculation in the limit of zero band gap (when the two atoms in the unit cell become identical) with a separate calculation for a body-centered-cubic (bcc) crystal. There is no ambiguity in sign for the bcc case.

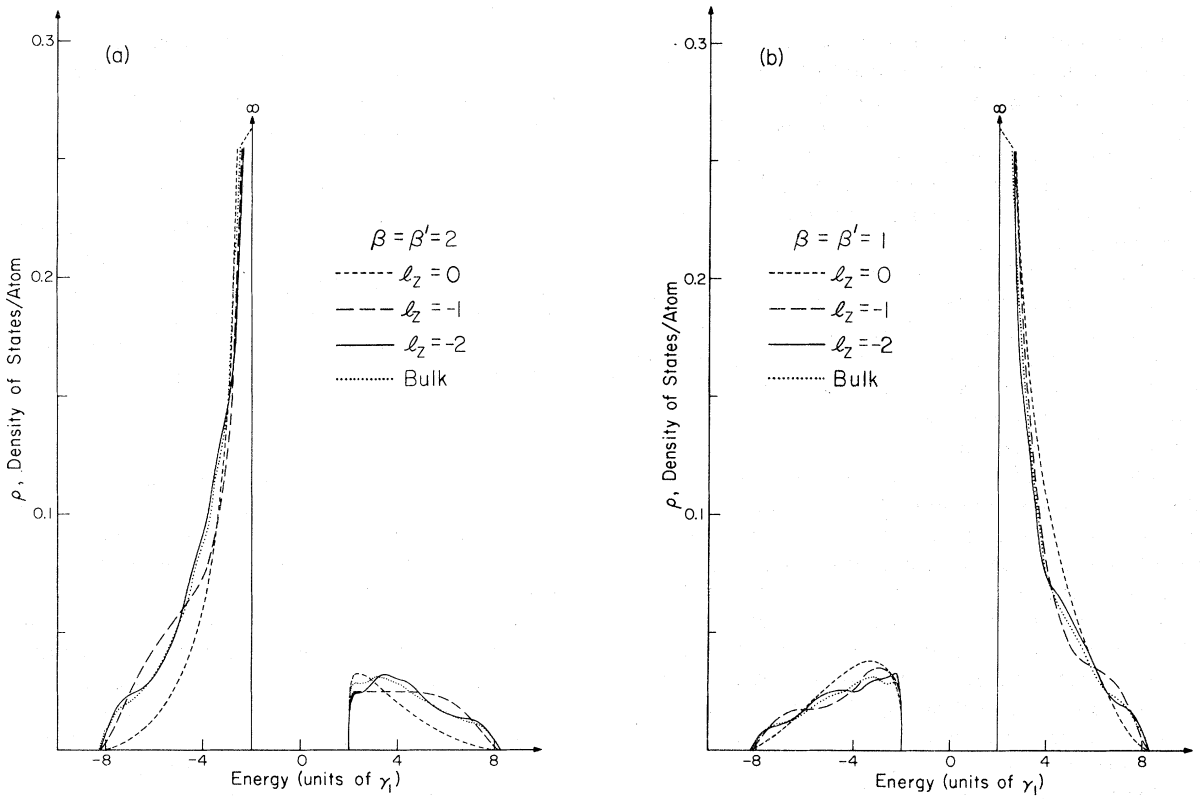

FIG. 12. Local density of states (per unit energy) per surface atom for the first six layers of atoms in the lower surface of Fig. 1. (a) Results for atoms of type 2 and (b) results for atoms of type 1. The local density of states for layers in the bulk are shown for comparison.

The sign which is given for Imt, then, is based on the assumption that there is a continuous change in the phase shift in going from the zero band gap case to the case with finite band gap. In the Appendix we show explicitly how this is done for the calculation of the partial phase shift discussed in Sec. III.

In Fig. 12 we show the local density of states (LDS) calculated numerically by sampling the surface Brillouin zone and evaluating Eq. (77). From the form of the surface Green's functions in Eqs. (78)–(81), the LDS for the upper surface in Fig. 1 is the mirror image of the LDS for the lower surface. This means, for example, that the LDS for the layer $l_z=1, \beta=1$ is the same as the LDS for the layer $l_z=0, \beta=2$ when the energy axis E is changed to $-E$. For this reason we only show the LDS for layers in the lower surface.

In Fig. 12(a) we show the LDS for atoms of type 2 representing the first, third, and fifth layer of atoms from the surface and for a layer in the bulk. In Fig. 12(b) we show the LDS for atoms of type 1 corresponding to the second, fourth, and sixth layer of atoms along with the LDS for a layer in the bulk. From these curves we see that the density of states at the surface is considerably more narrow in energy than the bulk density of states. This feature of band narrowing has been demonstrated theoretically for metals[32,54] and has been observed using photoemission.[55] Here we have demonstrated that band narrowing also occurs for semiconductors. Experimentally, the observed photoemission bandwidths for a large number of semiconductors are more narrow for ultraviolet photoemission spectra (UPS) than for x-ray photoemission spectra (XPS).[56] This trend can be interpreted as being due to band narrowing at the surface since the escape depth of electrons in UPS is smaller than for XPS.

In addition, from Fig. 12 we see that the density of states for the surface layers rapidly approaches the bulk density of states as we move into the crystal from the surface. By the fifth layer, the LDS is very similar to the bulk density of states.

V. CONCLUSIONS

We have obtained, for the first time, analytic expressions for both the bulk Green's function and the (001) surface Green's function of a two-band

model crystal of the CsCl structure. These Green's functions are significant because, in addition to studying the properties presented in this paper, they can serve as a starting point for calculations of both surface reconstruction and chemisorption on semiconductors and insulators. These two vital problems have not yet been examined from the Green's-function point of view. The fact that the Green's functions are analytic is important because it is then possible to study the surface using only simple numerical calculations, and consequently, it is much easier to understand how the results depend on the model parameters. This feature is often missing from more elaborate numerical calculations.

We have calculated the change in the density of electronic states caused by the creation of the surface for three separate models. The three models were chosen because one results in no surface states, one results in Shockley surface states, and one results in Tamm surface states. The existence conditions for these surface states is significantly different from those obtained previously, both in one-dimensional models and in one-band three-dimensional models. The change in the density of states shows both the addition of the derived surface states and, equally important, the concomitant perturbation of the infinite crystal density of states. In addition, we have used the change in the density of states to calculate various thermodynamic properties of the semiconductor or insulator surface, namely, the electronic specific heat and the surface electronic entropy. We have found, in contrast to one-band metals, that the surface specific heat falls to zero exponentially at low temperatures.

We have presented the local densities of states for a few layers of atoms in the surface region for the case when there are no surface states. We expect the results to be qualitatively the same for the other two models. We have shown, as is true for one-band crystals, that the band widths of the densities of states on the surface layers are more narrow than for the bulk layers. This fact can explain some of the discrepancies which have appeared between the results of UPS and XPS studies on semiconductor surfaces.

Finally, whereas the work in this paper is concerned with a specific surface of a specific structure of a two-band crystal, we believe that the qualitative features of the results are quite general and are common to all semiconductor and insulator surfaces. This belief is supported by analogy to the fact that for one-band metals, the model results for three faces of a simple cubic crystal, two faces of a body-centered-cubic crystal, and one face of a face-centered-cubic crystal are all qualitatively the same. Thus we believe that the results in this paper can serve as a general basis for the way in which one views both semiconductor and insulator surfaces.

ACKNOWLEDGMENTS

We acknowledge, with gratitude, support of this research by the National Science Foundation (Grant No. GK-43433), the IBM Corporation via a postdoctoral research fellowship (S.L.C.), and the National Science Foundation via an undergraduate research participantship (W.H.).

APPENDIX

We present here the calculation of the partial phase shift for the case of zero band gap by two different methods. For the first method, we set $E_1 = E_2 = 0$ in the derivation of the bulk Green's function of Sec. II to get the Green's function appropriate for a bcc crystal. We then obtain an analytic expression for the partial phase shift which contains no sign ambiguity. For the second method, we use the partial phase shift expression given in Sec. III and evaluate them in the limit $E_1 \to E_2 \to 0$. By comparing the two results, the sign ambiguity is removed for model I. The same method has been used for models II and III, and for the surface Green's function in Sec. IV.

Setting $E_1 = E_2 = \gamma_2 = 0$ in Eqs. (31)–(35), we find that each of the Green's functions, when written in integral form [using Eq. (36)], contains the factor $E/(E^2 - F^2)$. This factor can be split into partial fractions as

$$2E/(E^2 - F^2) = 1/(E+F) + 1/(E-F) \,. \tag{A1}$$

Using this identity and the integral from Eq. (37), we obtain for the bcc bulk-crystal Green's functions

$$G^{(0)}(l_z\beta, l_z'\beta, \vec{\phi}_s, E) = P'\tau^{2|l_z - l_z'|+1}, \quad \beta = 1, 2 \,, \tag{A2}$$

$$G^{(0)}(l_z 1, l_z' 2, \vec{\phi}_s, E) = -P'\tau^{|2(l_z - l_z')-1|+1}\chi^*(\vec{\phi}_s) \,, \tag{A3}$$

$$G^{(0)}(l_z 2, l_z' 1, \vec{\phi}_s, E) = -P'\tau^{|2(l_z - l_z')+1|+1}\chi(\vec{\phi}_s) \,, \tag{A4}$$

where

$$P' = 1/f(\tau^2 - 1) \,, \tag{A5}$$

$$\tau = \begin{cases} s - (s^2-1)^{1/2}, & s > 1 \,, \\ s + i(1-s^2)^{1/2}, & -1 < s < 1 \,, \\ s + (s^2-1)^{1/2}, & s < -1 \,, \end{cases} \tag{A6}$$

$$s = -E/2f \,, \tag{A7}$$

and where f is given by Eq. (46) and $\chi(\vec{\phi}_s)$ is given by Eq. (60).

Using the perturbation matrix for model I, Eq. (59), the Fredholm determinant in Eq. (54) reduces to the simple expression

$$D(\vec{\phi}_s, E) = -1/(\tau^2 - 1) . \quad \text{(A8)}$$

Inside the band, the magnitude of s [Eq. (A7)] is less than unity. Thus, using Eq. (A6) in Eq. (A8) and calculating the partial phase shift in Eq. (56) we obtain

$$\eta(\vec{\phi}_s, E) = -\arg[s/(1 - s^2)^{1/2}] . \quad \text{(A9)}$$

There is no ambiguity in the sign of the square root in this expression since the sign of the square root in Eq. (A6) is fixed.

In the second approach, we use the expressions for the bulk Green's functions given in Eqs. (39)–(42) and take the limit as $E_1 = E_2 = \gamma_2 = 0$. Again, the Fredholm determinant in Eq. (54) can be written analytically with the result

$$D(\vec{\phi}_s, E) = -1/(t - 1) , \quad \text{(A10)}$$

where t is given by Eq. (38). Inside the bands, we have

$$t = \xi + i(1 - \xi^2)^{1/2} , \quad \text{(A11)}$$

and the parameter ξ [from Eq. (47)] can be related to s [Eq. (A7)] by

$$\xi = 2s^2 - 1 . \quad \text{(A12)}$$

Substituting for t in Eq. (A10), we obtain

$$D(\vec{\phi}_s, E) = \tfrac{1}{2}[1 + i(1 - \xi^2)^{1/2}/(1 - \xi)] . \quad \text{(A13)}$$

The partial phase shift thus becomes

$$\eta(\vec{\phi}_s, E) = -\arg[(s^2)^{1/2}/(1 - s^2)^{1/2}] . \quad \text{(A14)}$$

The ambiguity in sign lies in the numerator of the argument since s can be negative. By comparison with Eq. (A9) we see that the positive root is the correct root. Thus, the numerator always has the sign opposite in sign to the energy E [note f is always positive in Eq. (A7)]. We assume from continuity that this sign convention is valid even when the band gap is not zero and when the partial phase shift cannot be obtained analytically.

---

*Work partially supported by National Science Foundation Grant No. GK-43433.

†National Science Foundation Undergraduate Research Participant.

‡IBM Postdoctoral Research Fellow.

[1]W. Ho, S. L. Cunningham, W. H. Weinberg, and L. Dobrzynski, Phys. Rev. B (to be published).
[2]J. Koutecky, Adv. Chem. Phys. 9, 85 (1965).
[3]S. G. Davison and J. D. Levine, Solid State Phys. 25, 1 (1970).
[4]E. T. Goodwin, Proc. Cambridge Philos. Soc. 35, 221 (1939).
[5]T. A. Hoffmann and A. Konya, Acta. Physica Hung. 1, 5 (1951).
[6]T. A. Hoffmann, Acta Physica Hung. 1, 175 (1951).
[7]A. T. Amos and S. G. Davison, Physica (Utr.) 30, 905 (1964).
[8]S. G. Davison and J. Koutecky, Proc. Phys. Soc. Lond. 89, 237 (1966).
[9]J. D. Levine and S. G. Davison, Phys. Rev. 174, 911 (1968).
[10]S. L. Cunningham and A. A. Maradudin, Phys. Rev. B 7, 3870 (1973).
[11]J. Koutecky and M. Tomasek, Phys. Rev. 120, 1212 (1960).
[12]See, for example, R. O. Jones, J. Phys. C 5, 1615 (1972); F. Yndurain and M. Elices, Surf. Sci. 29, 540 (1972).
[13]E. T. Goodwin, Proc. Cambridge Philos. Soc. 35, 232 (1939).
[14]D. Pugh, Phys. Rev. Lett. 12, 390 (1964).
[15]K. Hirabayashi, J. Phys. Soc. Jpn. 27, 1475 (1969).
[16]I. Alstrup, Surf. Sci. 20, 335 (1970).
[17]I. Alstrup, Phys. Status Solidi B 45, 209 (1971).
[18]K. C. Pandey and J. C. Phillips, Solid State Commun. 14, 439 (1974).
[19]K. C. Pandey and J. C. Phillips, Phys. Rev. Lett. 32, 1433 (1974).
[20]J. D. Joannopoulos and M. L. Cohen, Phys. Lett. A 49, 391 (1974).
[21]See, for example, E. Caruthers, L. Kleinman, and G. P. Alldredge, Phys. Rev. B 9, 3325, 3330 (1974).
[22]G. R. Baldock, Proc. Cambridge Philos. Soc. 48, 457 (1952).
[23]G. F. Koster and J. C. Slater, Phys. Rev. 95, 1167 (1954).
[24]J. Koutecky and S. G. Davison, Int. J. Quant. Chem. 2, 73 (1968).
[25]J. Koutecky, Phys. Rev. 108, 13 (1957).
[26]B. W. Holland, Philos. Mag. 8, 87 (1963).
[27]R. A. Brown, Phys. Rev. 156, 889 (1967).
[28]M. Tomasek, in *The Structure and Chemistry of Solid Surfaces*, edited by G. A. Somorjai (Wiley, New York, 1969).
[29]S. Freeman, Phys. Rev. B 2, 3272 (1970).
[30]J. D. Levine and S. Freeman, Phys. Rev. B 2, 3255 (1970). More recently, D. Lohez and M. Lannoo [J. Phys. 35, 647 (1974)] have studied the same system by means of the resolvent technique using a more complicated model. They obtain the bulk Green's functions in analytic form.
[31]A. van der Avoird, S. P. Liebmann, and D. J. M. Fassaert, Phys. Rev. B 10, 1230 (1974).
[32]D. Kalkstein and P. Soven, Surf. Sci. 26, 85 (1971).
[33]S. M. Bose and E-Ni Foo, Phys. Rev. B 10, 3534 (1974).
[34]B. S. DeWitt, Phys. Rev. 103, 1565 (1956).
[35]A. Blandin, J. Phys. Radium 22, 507 (1961).

[36]G. Toulouse, Solid State Commun. 4, 593 (1966).
[37]G. Allan, Ann. Phys. (Paris) 5, 169 (1970).
[38]G. Allan and P. Lenglart, Surf. Sci. 15, 101 (1969).
[39]G. Allan and P. Lenglart, Surf. Sci. 30, 641 (1972).
[40]T. L. Einstein, Surf. Sci. 45, 713 (1974).
[41]T. L. Einstein and J. R. Schrieffer, Phys. Rev. B 7, 3629 (1973).
[42]J. R. Schrieffer, J. Vac. Sci. Technol. 9, 561 (1972).
[43]T. B. Grimley and C. Pisani, J. Phys. C 7, 2831 (1974).
[44]J. M. Ziman, *Principles of the Theory of Solids* (Cambridge U. P., Cambridge, England, 1965), Chap. 5.
[45]D. N. Zubarev, Usp. Fiz. Nauk 71, 71 (1960) [Sov. Phys. Usp. 3, 320 (1960)].
[46]A. A. Maradudin, E. W. Montroll, G. H. Weiss, and I. P. Ipatova, *Theory of Lattice Dynamics in the Harmonic Approximation*, 2nd ed. (Academic, New York, 1971), Suppl. 3, Chap. 2.
[47]L. Dobrzynski, Ann. Phys. (Paris) 4, 637 (1969).
[48]If we had included the other second-neighbor interaction, $\gamma_2^{(1)}$, the denominator in the integral would be quadratic in $\cos\phi_z$ rather than linear.
[49]The phase shift jumps to $-\pi$ rather than $+\pi$ because we use the retarded Green's functions. The factor $i\epsilon$ tells us we must circle the singularity in the upper-half of the complex plane resulting in a change of phase of π. However, the phase shift is the negative of the change of phase; therefore we get a jump of $-\pi$.
[50]S. L. Cunningham, Phys. Rev. B 10, 4988 (1974).
[51]J. Friedel, Nuovo Cimento Suppl. 7, 287 (1958).
[52]L. Dobrzynski and D. L. Mills, Phys. Rev. B 7, 2367 (1973).
[53]S. L. Cunningham (unpublished) has been able to show that the "surface" Green's function for a finite diatomic chain where each atom has one orbital (two orbitals per unit cell) can also be expressed as a simple linear combination of "bulk" Green's functions.
[54]R. Haydock and M. J. Kelly, Surf. Sci. 38, 139 (1973).
[55]See, for example, N. E. Christensen and B. Feuerbacher, Phys. Rev. B 10, 2349 (1974); *ibid.* 10, 2373 (1974).
[56]See, for example, D. E. Eastman, W. D. Grobman, J. L. Freeouf, and M. Erbudak, Phys. Rev. B 9, 3473 (1974).